NEW HORIZONS AND OLD PITFALLS IN FREQUENCY AND TIME METROLOGY

F. L. Walls

Frequency & Time Standards Section
National Bureau of Standards
Boulder, Colorado USA

Since the first Symposium on Frequency Standards and Metrology in 1971, there have been many significant advances in time and frequency metrology. I will describe the present state-of-the-art, indicate some problem areas, and attempt to forecast some future advances in a few areas. Specifically, I want to cover the measurement of stability of precision oscillators and signal handling equipment in frequency and time domain, new developments in oscillators which show very high spectral purity, or good short-term stability, techniques for combining two or more frequency determining elements into a superior frequency standard system, and make a few comments about some new understandings and advancements in frequency multiplication.

Figure 1 shows state-of-the-art short-term and medium-term stability of various classes of frequency standards. Perhaps one of the most notable things is not the introduction of so many new standards since 1971, but the outstanding improvements in some of the old ones, e.g. quartz oscillators.

Systems and techniques for the measurement of stability in frequency and time domain are the tools that allow us to characterize oscillators and signal handling equipment. Equally important, these techniques are used as diagnostic tools to improve existing devices and to design intelligent uses of frequency standards in systems applications. Frequency domain measurements and characterization of stability via $S_y(f)$, spectral density of frequency fluctuations, or $S_\phi(f)$, the spectral density of phase fluctuations, are some of the most powerful tools that we have in evaluating types and levels of fundamental noise processes in oscillators and signal handling equipment, as they allow us to examine individual Fourier components of residual frequency or phase modulation. Also, the time domain stability is uniquely defined for any given bandwidth from the frequency domain measurements. The inverse is not always true, in that we cannot uniquely transfer back from time domain variance measurements to frequency domain because the variance measurements are actually an average over the different Fourier components that contribute to the time domain stability.

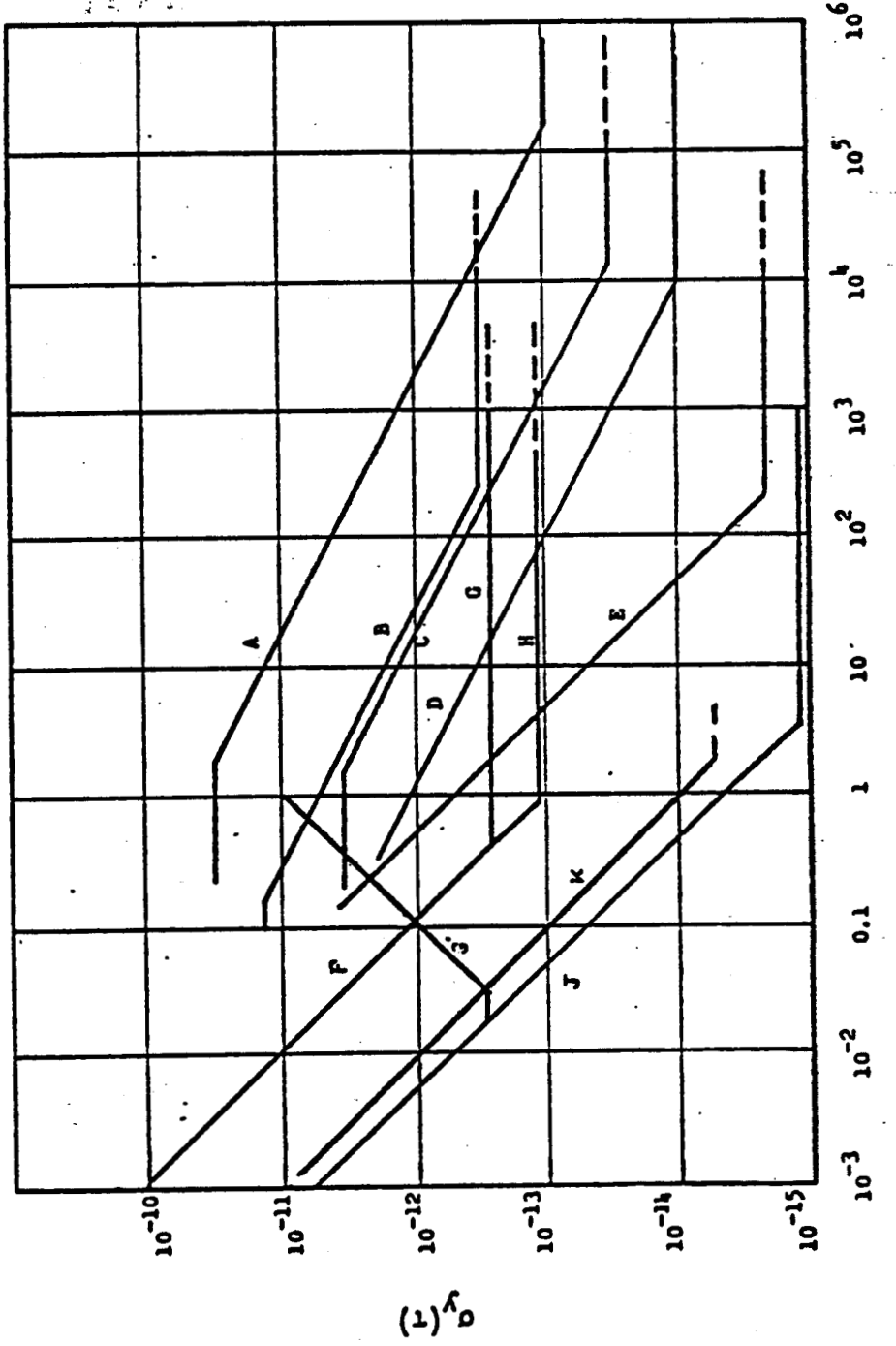
$\sigma_y(\tau)$
10^{-10}
10^{-11}
10^{-12}
10^{-13}
10^{-14}
10^{-15}
10^{-3}
10^{-2}
0.1
1
10^{1}
10^{2}
10^{3}
10^{4}
10^{5}
10^{6}
SAMPLE TIME τ(s)
A
B
C
D
E
F
G
H
J
K

FIGURE 1

Figure 2 shows a typical scheme which is used for measuring spectral density of phase fluctuations in the range from 1 MHz to perhaps 10 GHz [1]. Analogs of this scheme are used up to the visible. The source is shown as a simple oscillator, however, it might actually be an oscillator plus an amplifier or a frequency multiplier. In order to obtain precision measurements of $S_y(f)$ or equivalently, $S_\phi(f)$, the residual amplitude and frequency modulation or phase modulation must be small so that the carrier is well-defined and further, we must suppress the residual amplitude modulation from the measurement. In the past, it has often been assumed that amplitude modulation is small compared to phase modulation in precision sources. This is in fact not true over the major portion of the spectrum of precision oscillators. If additive noise processes are present, they will contribute an equal amount to amplitude and phase modulation. We can take advantage of this as a diagnostic tool, because it allows us to distinguish between fundamental noise processes which are additive, and noise processes which are multiplicative or produced by direct modulation of the frequency. In fact, if the oscillators under test in Figure 2 are free-running, we will measure the spectral density of phase fluctuations when the signals are in quadrature at the mixer, and when they are in phase, we will measure the amplitude spectrum. This can be very useful as a diagnostic tool, as I mentioned before.

Frequency domain analysis can also be done using time domain sampling of the phase or frequency difference between two oscillators and computing $S_\phi(f)$ or $S_y(f)$ using fast Fourier transforms or the Hadamard variance [2].

Figure 3 shows the block diagram of a new approach to using the Hadamard variance [3]. Its main advantage is that one can easily measure $S_y(f)$ from 0.001 Hz to 1 kHz without trouble from the spurious lobes of the Hadamard variance.

Figure 4 shows the kind of typical performance for $S_\phi(f)$ measurement floors that I think can be obtained with both systems, although these measurements were actually taken at 5 MHz with the scheme shown in Figure 2. One could expect to obtain performance of this order of magnitude from about 10 kHz out to about 1 GHz. Beyond about 10 GHz, most of the measurements are a combination of amplitude and phase spectra.

PHASE NOISE MEASUREMENT SYSTEM

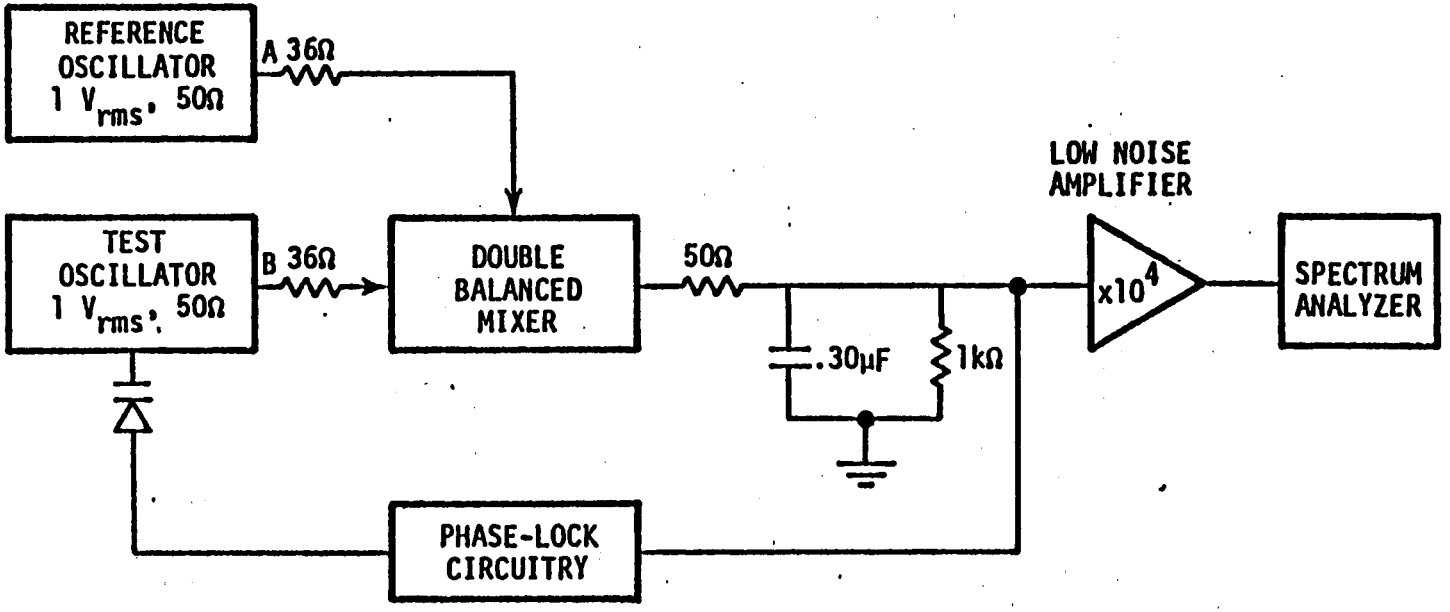

FIGURE 2

The noise added by signal processing equipment can be measured by replacing the test oscillator in Figure 2 by a 90° phase shifter, driven from the reference oscillator, eliminating the phase lock circuitry, and placing the component under study at Point A or B. In this case, the residual phase modulation in the source oscillator cancels out to a very high degree, perhaps as much as 60 dB if the bandwidths of both channels are very similar. This scheme allows one to measure noise in components down to the resolution of the measurement system which essentially is limited by the added noise of the mixer and dc amplifiers and is usually independent of what the source oscillator happens to be. There are a number of amplifiers and oscillators and signal handling equipment which have noise in the so-called white phase region which are uncomfortably close to the measurement floor of Figure 2, which is $S_\phi(f) = 2.5 \times 10^{-18}$ rad^2/Hz.

One possible solution to this measurement problem is the phase noise measurement system shown in Figure 5. It consists of 2 conventional phase noise channels which are nearly identical [1].

At the output of each double balanced mixer there is a signal which is proportional to the phase difference, $\Delta\phi$, between the two oscillators and a noise term, V_n, due to contributions from the mixer and amplifier. The voltages at the input of each bandpass filter are

$$V_1 = A_1 \Delta\phi(t) + C_1 V_{n1}(t)$$

$$V_2 = A_2 \Delta\phi(t) + C_2 V_{n2}(t)$$

where $V_{n1}(t)$ and $V_{n2}(t)$ are substantially uncorrelated. Each bandpass filter produces a narrow band noise function around its center frequency f:

$$V_1(\text{BP filter output}) = A_1[S_\phi(f)]^{1/2} B_1^{1/2} \cos[2\pi ft + \Psi(t)] + C_1[S_{V_{n1}}(f)]^{1/2} B_1^{1/2} \cos[2\pi ft + n_1(t)]$$

$$V_2(\text{BP filter output}) = A_2[S_\phi(f)]^{1/2} B_2^{1/2} \cos[2\pi ft + \Psi(t)] + C_2[S_{V_{n2}}(f)]^{1/2} B_2^{1/2} \cos[2\pi ft + n_2(t)]$$

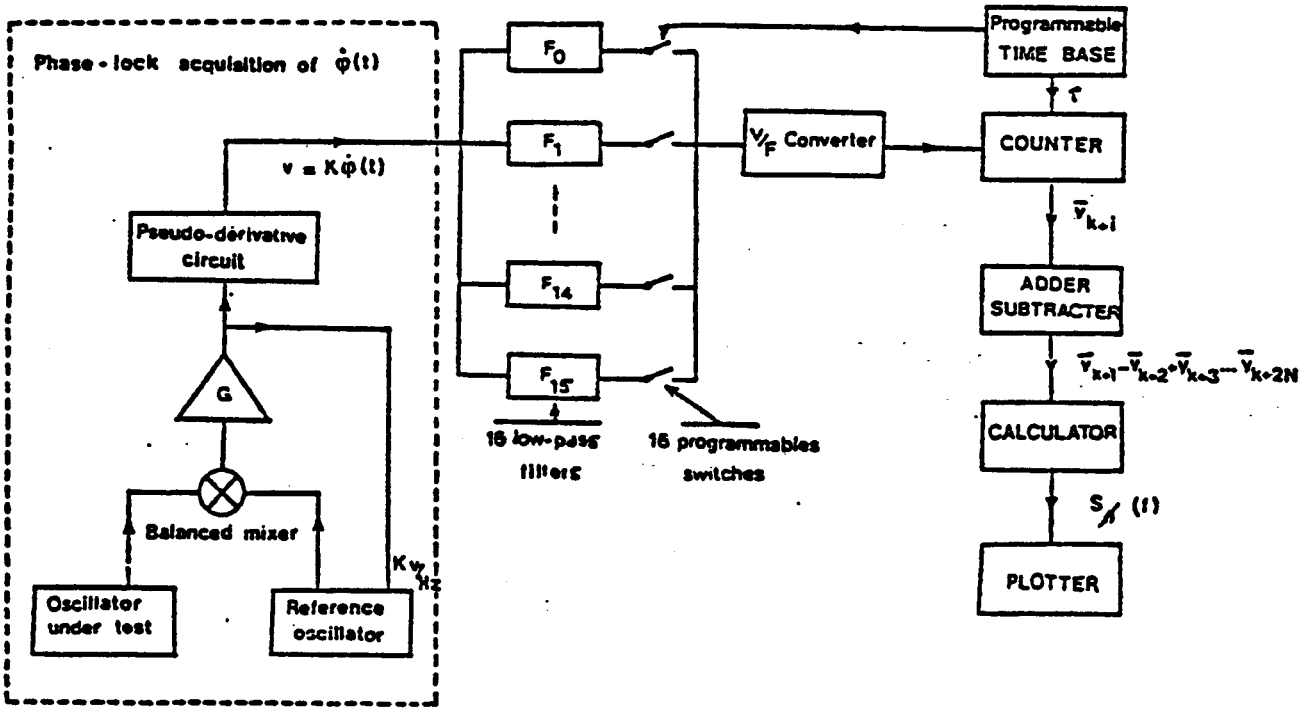

FIGURE 3

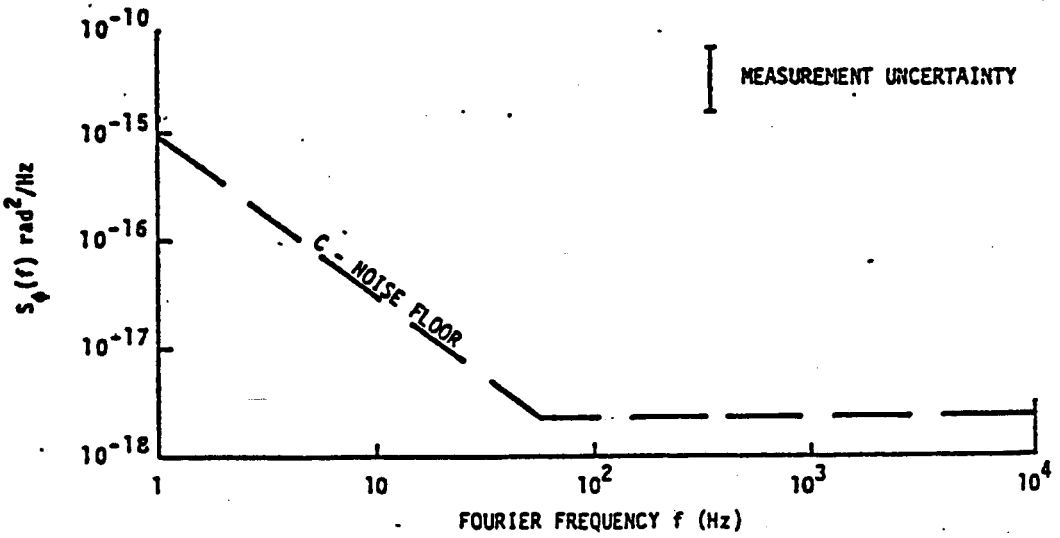

FIGURE 4

PHASE NOISE MEASUREMENT SYSTEM USING CORRELATION TECHNIQUE

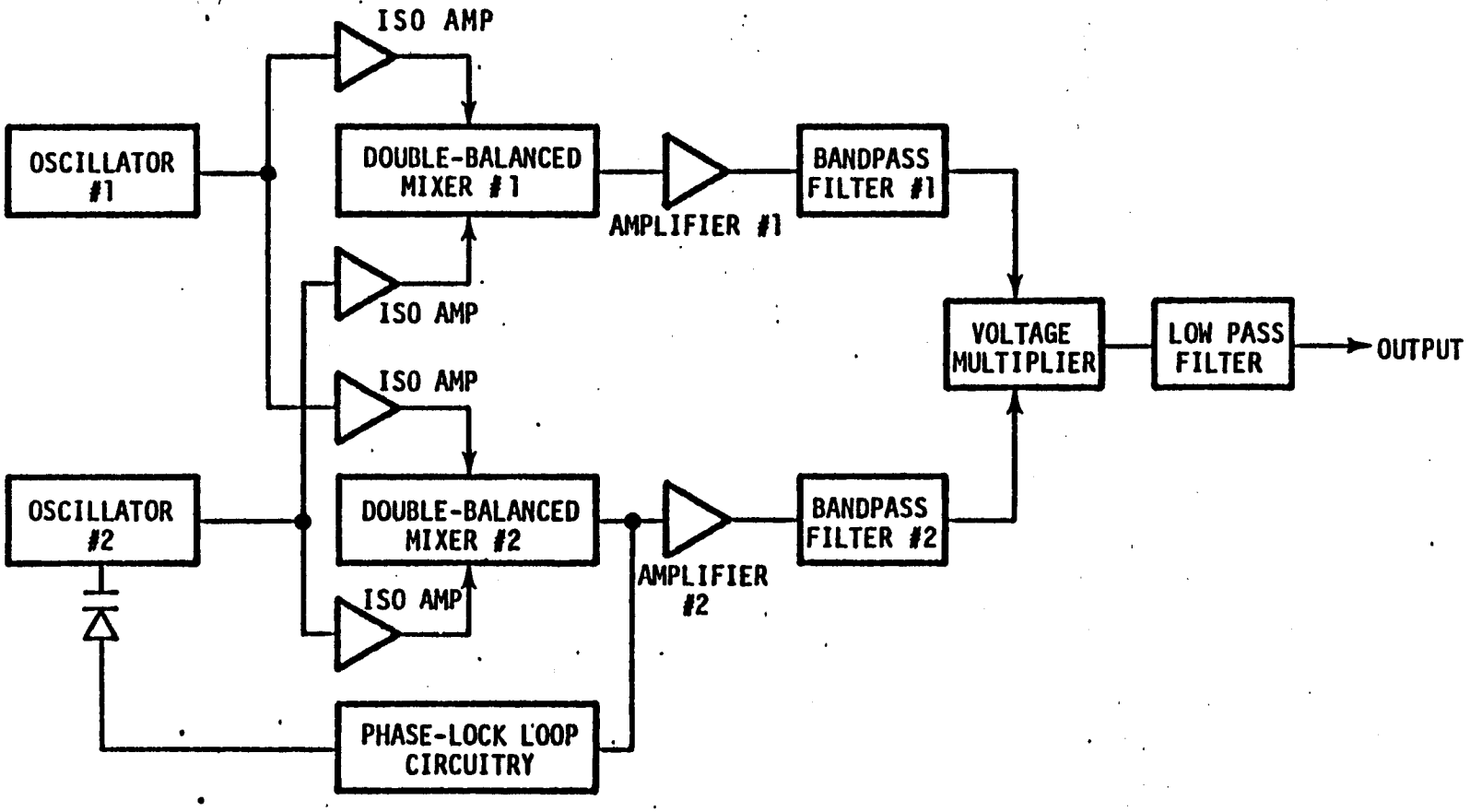

FIGURE 5

where B_1 and B_2 are the equivalent noise bandwidths of filters 1 and 2 respectively. Both channels are bandpass filtered in order to help eliminate aliasing and dynamic range problems. The phases $\Psi(t)$, $\eta_1(t)$ and $\eta_2(t)$ take on all values between 0 and 2π with equal likelihood. The output of the correlator, which is a wideband, four quadrant multiplier, consists of a dc term proportional to $S_\phi(f)$ between the two oscillators plus an ac term which is averaged to near zero

$$V_{out} = 1/2\ A_1 A_2 S_\phi(f)\ B_1^{1/2}\ B_2^{1/2} + \text{ac terms}$$

Preliminary measurements at 5 MHz show that one can reach noise floors for $S_\phi(f)$ below 10^{-20} rad^2/Hz at Fourier frequencies above 10 kHz. Although further improvements on the correlation technique for making phase noise measurements are surely feasible, the present performance level appears sufficient to measure the next generation of oscillators and signal handling equipment as well as present ones.

Time domain measurements expressed in the pair variance (Allan Variance) as in Figure 1 are the most common way to characterize stability of precision oscillators.This method of measurement generally requires looking at the accumulated phase difference between the two oscillators under test. The most commonly used system is the so-called hetrodyne frequency method or beat-frequency method shown in Figure 6 where the time between zero crossings is counted and recorded with a printer. One of the major limitations of this system is that it is restricted to measurement times which are longer than 1 beat period. One early attempt to get around this difficulty is shown in Figure 7. The output voltage of the mixer is proportional to the frequency difference between the two oscillators for times which are much longer than the attack time of the phase-lock loop. This voltage is then usually converted to a frequency and its stability measured. The limitation on the shortest measurement time is determined by the speed of the phase lock loop or the maximum rate of the voltage to frequency converter. This system also features the low noise of the hetrodyne system.

Very recently there has been a major improvement in time domain measurements with the introduction of the dual mixer time domain measurement system shown in Figure 8. In this method a transfer oscillator which can be offset from the two oscillators is used to obtain the desired beat frequency. The beat

frequency is usually adjusted to be only slightly larger than the smallest inverse measurement time desired. By adjusting the phase shifter, the time between the zero crossings of the two beat frequencies can be made very small compared with the beat period. Then the phase noise in the transfer oscillator cancels out to a very high degree.

Figure 9 shows typical results for the noise floor for $\sigma_y(\tau)$ for (a) the hetrodyne method and (b) the dual mixer time difference method. Noise bandwidth is 1 kHz. Noise considerations indicate that the dual mixer system could achieve $6 \times 10^{-15}\ \tau^{-1}$. Measurement times of 10^{-6} sec could be realized at some sacrifice in noise floor. The hetrodyne method could achieve $4 \times 10^{-15}\ \tau^{-1}$ using the noise floor shown in Figure 4.

Now, in all stability measurements between oscillators, one has to be very careful to avoid injection locking. With the aid of the following equation, we can get a rough idea of the order of magnitude of the frequency separation required between the oscillators under test to prevent injection locking, or equivalently an estimation of the required isolation between the two oscillators given a fixed frequency offset,

$$d\phi = 2.Q\ dy$$

where $d\phi$ represents the phase shift across a single resonant circuit of quality factor Q, when the applied frequency is fractionally offset from resonance by an amount equal to dy. If we apply this grossly over simplified model to an oscillator with quality factor Q, we see that the effect of introducing an additional phase shift within the oscillating loop is to pull the fractional frequency by an amount

$$dy = \frac{d\phi}{2Q} .$$

Suppose that you had 2 frequency standards containing frequency determining elements with quality factors of 1×10^{8} which are offset 1×10^{-13} in frequency. The amount of induced phase deviation required in order to make the standards lock up is of order 2Q dy or 2×10^{-5} radians. This means that an injected signal only 2×10^{-5} as large as the driving signal amplitude or 4×10^{-10} in power will cause the two oscillators to lock up. Therefore, in order to make reliable measurement of frequency stability,one is required to provide 100 dB or more isolation between the two frequency standards.Alternately, one could increase the frequency offsset. This

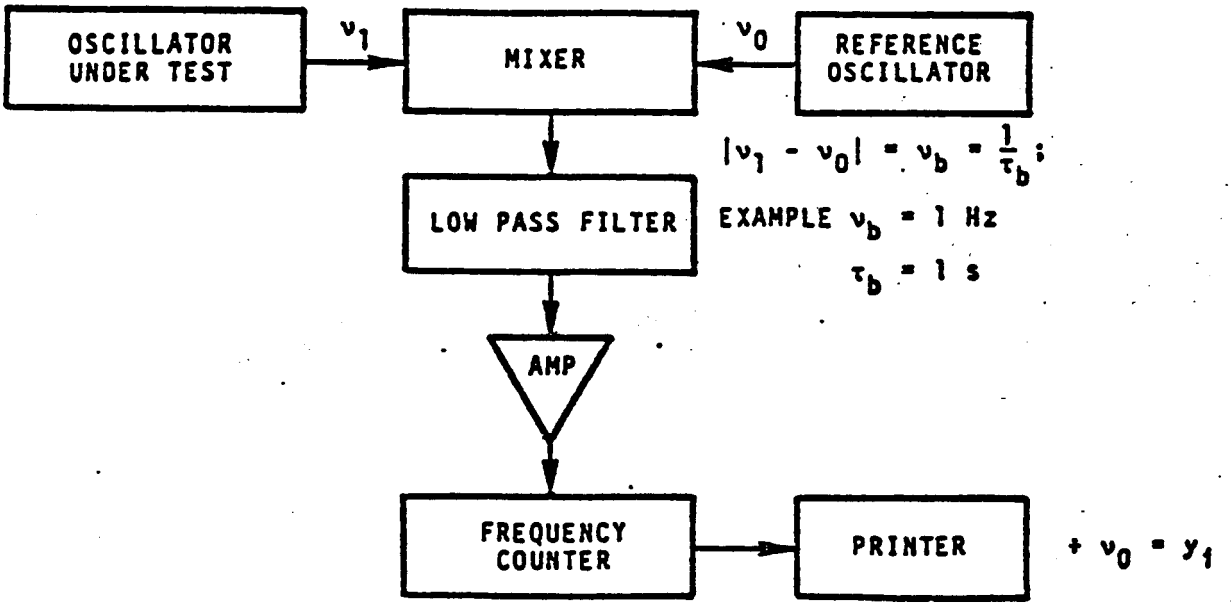

FIGURE 6

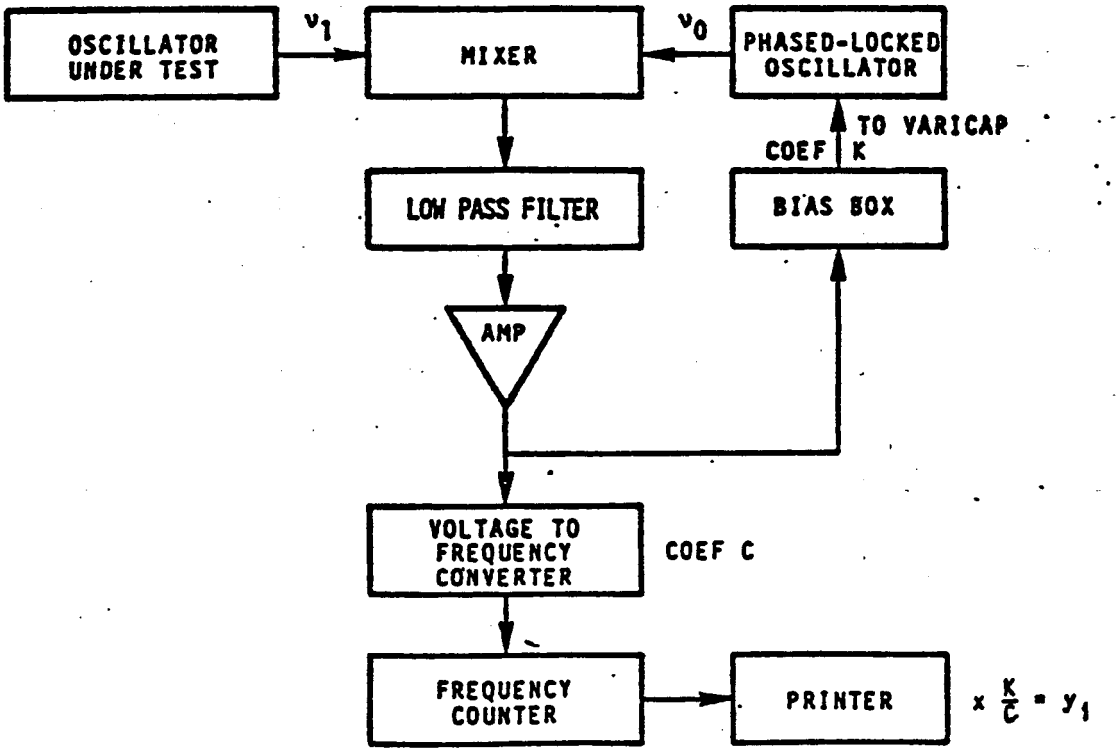

FIGURE 7

DUAL MIXER TIME DIFFERENCE SYSTEM

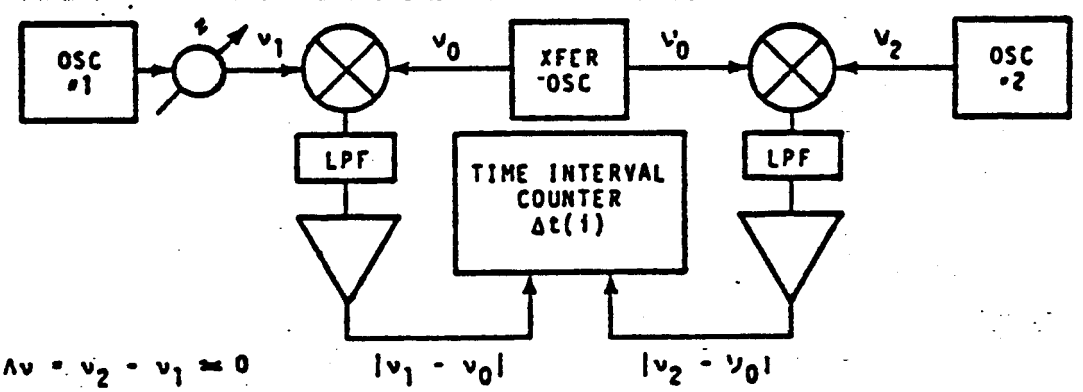

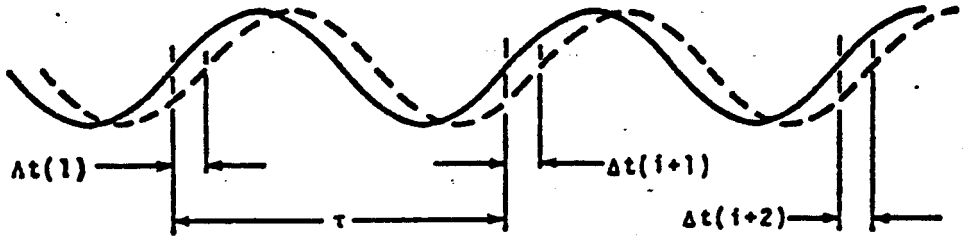

TIME DIFFERENCE: $x(i) = t_2 - t_1 = \frac{\Delta t(i)}{\tau\nu} - \frac{\phi}{2\pi\nu}$

FRACTIONAL FREQUENCY: $y(i) = \frac{\Delta\nu(i)}{\nu} = \frac{\Delta t(i+1) - \Delta t(i)}{\tau^2\nu}$

FIGURE 8

explains in essence, the reason why frequency stability measurements between very stable lasers where isolations are notoriously low, are often done via a second set of offset locked lasers.

Another problem often encountered in time domain measurements is the presence of bright lines. They might actually be in the oscillators under test or in the measurement system. Figure 10 illustrates such a problem. $\sigma_y(\tau)$ is shown for the case of an equal amount of 60 Hz phase modulation and white phase modulation. Note the very pronounced oscillation in $\sigma_y(\tau)$ vs. τ. If you were taking time domain measurements at different averaging times, you would obtain a rather strange looking plot, with a slope of almost $1/\tau$ but very bumpy. This is an indication of bright lines. The dual mixer time domain measurement system makes it easy to see the presence of bright lines; if you know where to look, as you can trace out the peaks and valleys. The valleys now correspond to $\sigma_y(\tau)$ without the bright lines. Note that the perturbation to $\sigma_y(\tau)$ due to a bright line falls as τ^{-1} independent of the slope of $\sigma_y(\tau)$ without the bright line. Of course, the most efficient way to detect the presence of bright lines is via the frequency domain stability either $S_\phi(f)$ or $S_y(f)$.

Next, I would like to just mention some very recent advances in oscillators which feature exceptionally good short-term stability or spectral purity. Curve a, Figure 11 shows the kind of quartz oscillator performance that we have been used to in the past, while curve b, Figure 11 shows the measured performance of a new 5 MHz quartz oscillator that has just appeared on the commercial market. It has a substantial improvement at large Fourier frequencies. This means that if this oscillator were used as a source for multiplication to the mm region or above, then the resulting signal-to-noise would be better(assuming a good multiplier chain). At low Fourier frequencies, the new oscillator is somewhat worse than the old one. The optimum solution, as we will see later, would be to phase-lock the new oscillator to the old one with a unity gain bandwidth of about 10 Hz or equivalently an attack time of $(1/20\pi)$ s. Curve c, Figure 11 shows the equivalent phase noise of the superconducting cavity stabilized oscillator at 5 MHz [5]. This system actually runs at 10 GHz. A new superconducting oscillator has been proposed which promises to yield approximately 60 dB reduction in the noise pedestal shown in Curve c [6]. Curve d, Figure 11 shows the approximate phase noise of the rubidium maser [7].

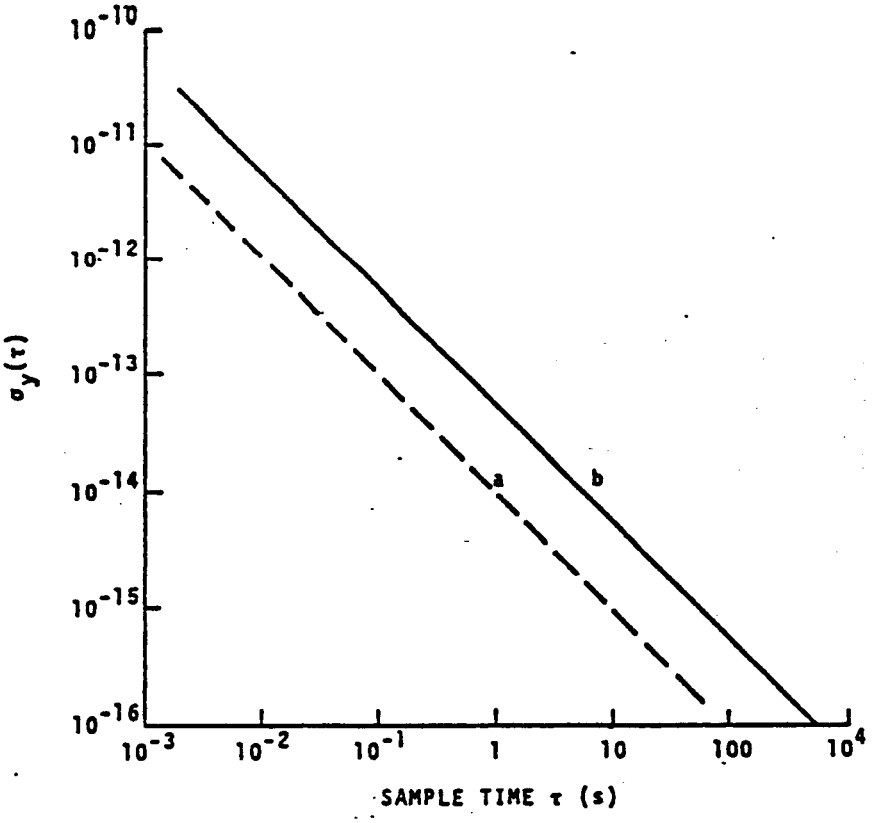

FIGURE 9

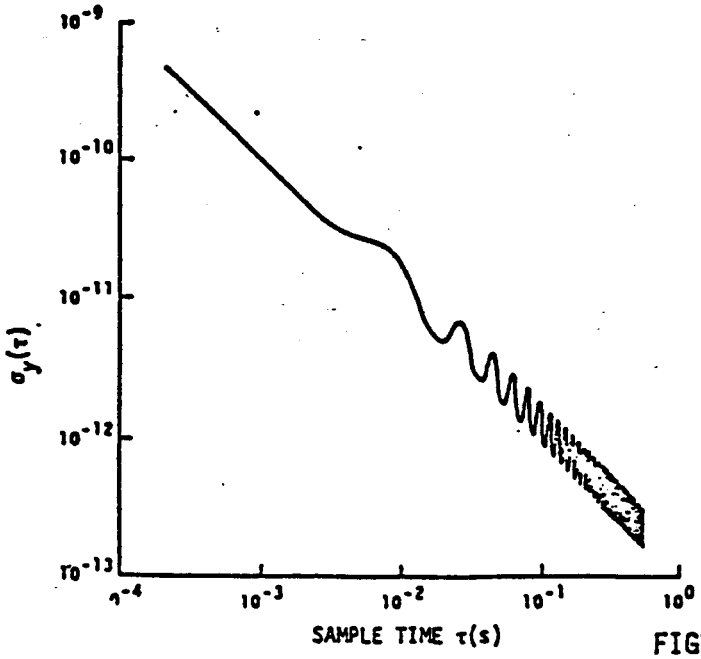

FIGURE 10

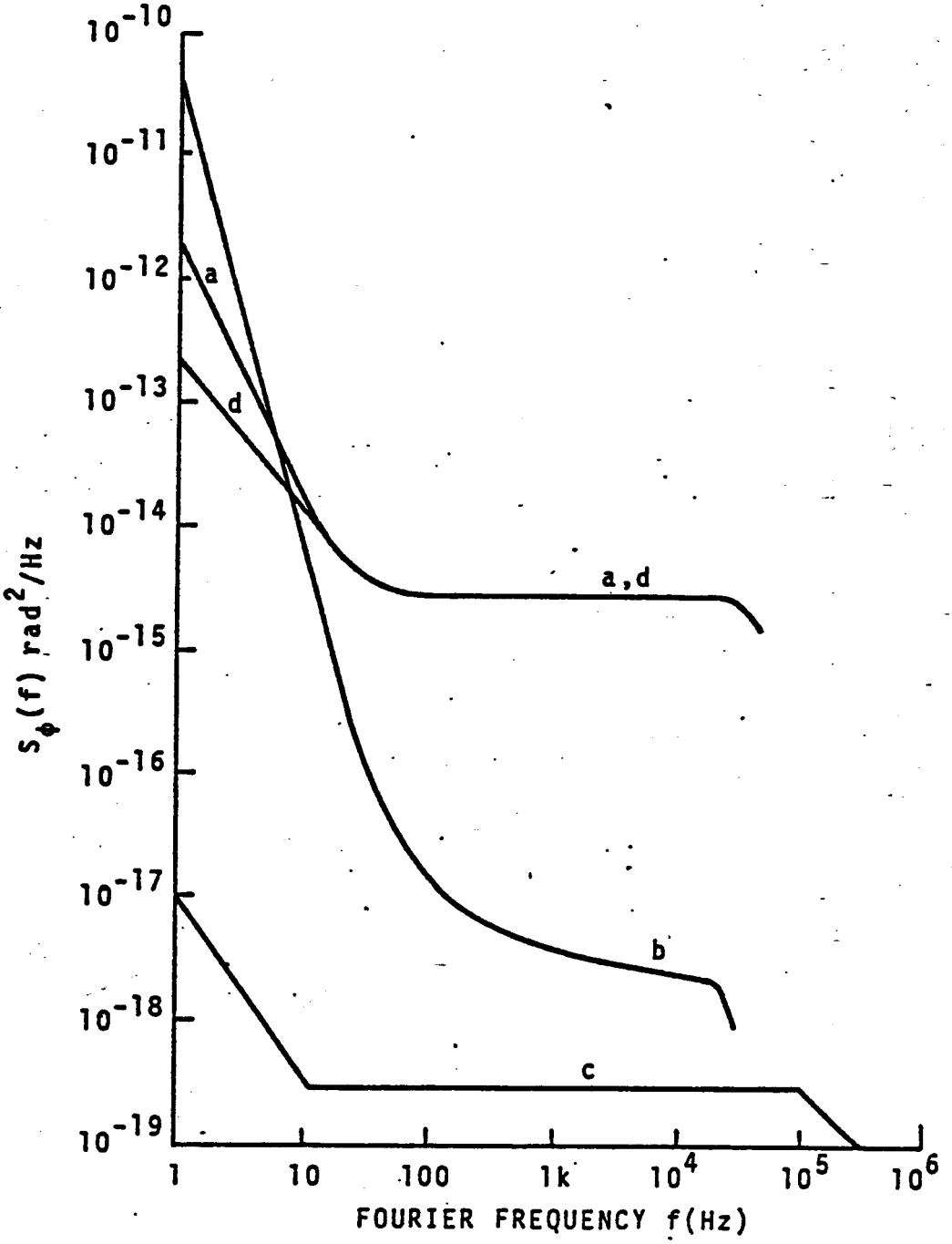
10^{-10}
10^{-11}
10^{-12}
10^{-13}
10^{-14}
10^{-15}
10^{-16}
10^{-17}
10^{-18}
10^{-19}
$S_\phi(f)$ rad^2/Hz
a
d
a,d
b
c
1
10
100
1k
10^4
10^5
10^6
FOURIER FREQUENCY f(Hz)

FIGURE 11

Next, I would like to spend some time discussing phase-lock loops, as they form an important and sometimes limiting link, in achieving ultimate performance from a given frequency standard system. We have all worked with systems in which the short-term stability is not determined by the same phenomenon that determines the long-term stability. Let me remind you that the proper frame of reference for calculating and comparing performance of the phase-lock loop, or frequency-lock loop is in frequency domain and not time domain because in fact the servo acts in frequency domain [1]. So assume that we have some kind of reference oscillator(it could even be a reference signal); a tunable VCO; a detector which could either work via phase or frequency; and a servo system. The spectral density of phase or frequency fluctuations, for the VCO locked to the reference is given by

$$S(f) = \left| \frac{G_{servo}(1/2\pi\tau)}{1+G_{servo}(1/2\pi\tau)} \right|^2 \left[S(f, ref) + S(f, n) + \frac{S(f, VCO)}{\left| G_{servo}(1/2\pi\tau) \right|^2} \right]$$

where $G_{servo}(f=1/2\pi\tau)$ is the measured servo gain, S(f, ref) is the spectral density of phase fluctuations $S_\phi(f)$ for a phase lock loop or the spectral density of frequency fluctuations $S_y(f)$ for a frequency lock loop of the reference signal, S(f, n) is the corresponding spectral density that would be required in the VCO to produce the servo system noise, and S(f, VCO) is the corresponding spectral density of phase or frequency fluctuations of the unlocked VCO.

Figure 12 illustrates this for various attack times where it has been assumed that G_{servo} varies as 6 dB/octave, and has a maximum gain of 10^4. The resulting time domain stability is shown in Figure 13. Note that changing the attack time from 10^{-4} to 10^{-6} seconds has little effect on the short-term stability. This is because the time domain stability, $\sigma_y(\tau)$, is essentially proportional to the integral of the total phase fluctuations [8]

$$\sigma_y(\tau) = k \int_{\frac{1}{2\pi\tau}}^{f_h=\infty} S_y(f)\, df$$

and in this example most of the phase fluctuation occurs at Fourier frequencies beyond the loop attack time. Only when $1/2\pi t_v$ (τ_v = loop attack time) exceeds the bandwidth of $S_\phi(f)$ does the time domain stability show significant improvements. The limited gain means that when the low frequency noise starts to increase due to drift, flicker of frequency or whatever, the output just tracks it at reduced levels.

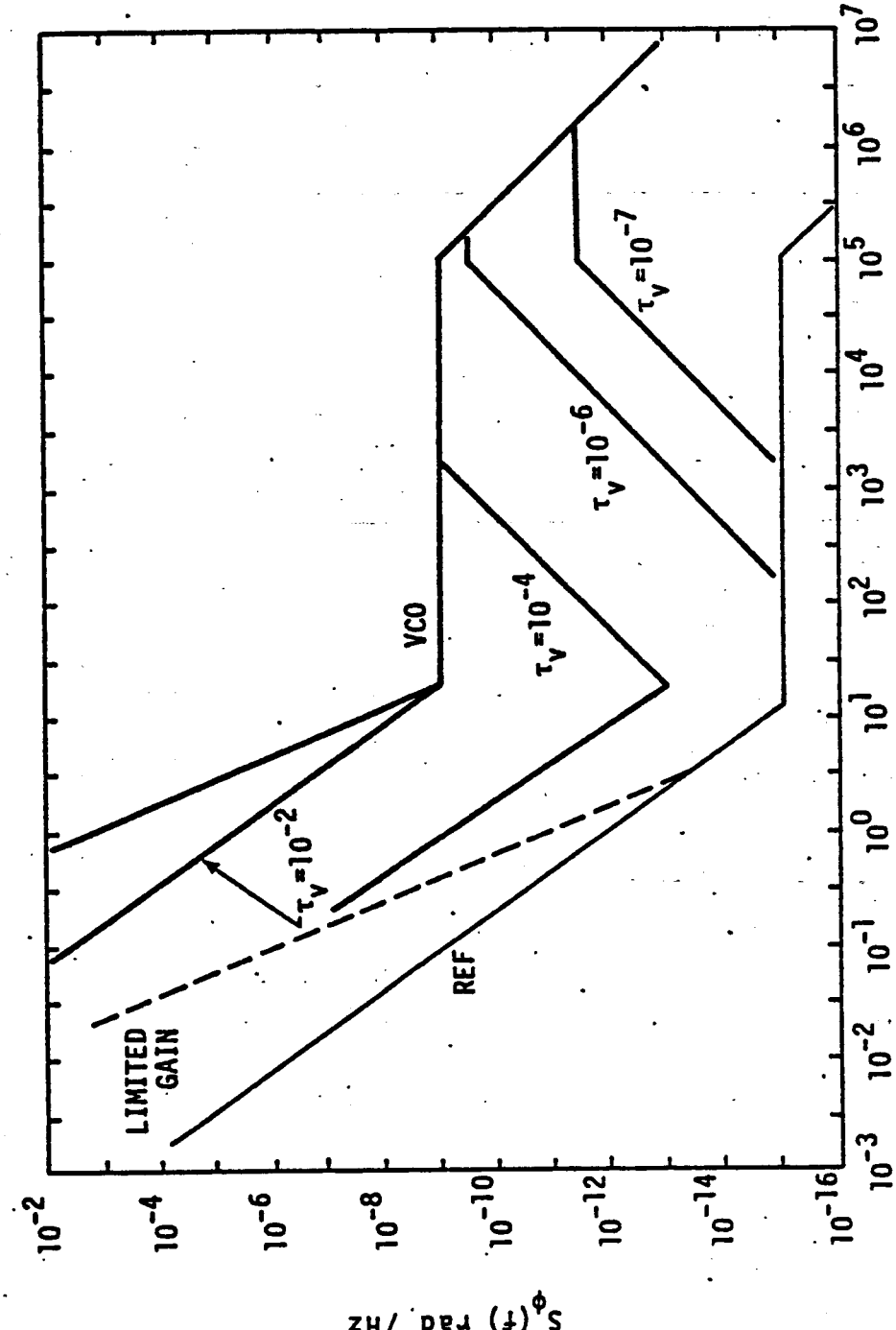
$S_\phi(f)$ rad^2/Hz
FOURIER FREQUENCY f (Hz)
VCO
REF
LIMITED GAIN
τ_v=10^{-2}
τ_v=10^{-4}
τ_v=10^{-6}
τ_v=10^{-7}
10^{-2}
10^{-4}
10^{-6}
10^{-8}
10^{-10}
10^{-12}
10^{-14}
10^{-16}
10^{-3}
10^{-2}
10^{-1}
10^{0}
10^{1}
10^{2}
10^{3}
10^{4}
10^{5}
10^{6}
10^{7}

FIGURE 12

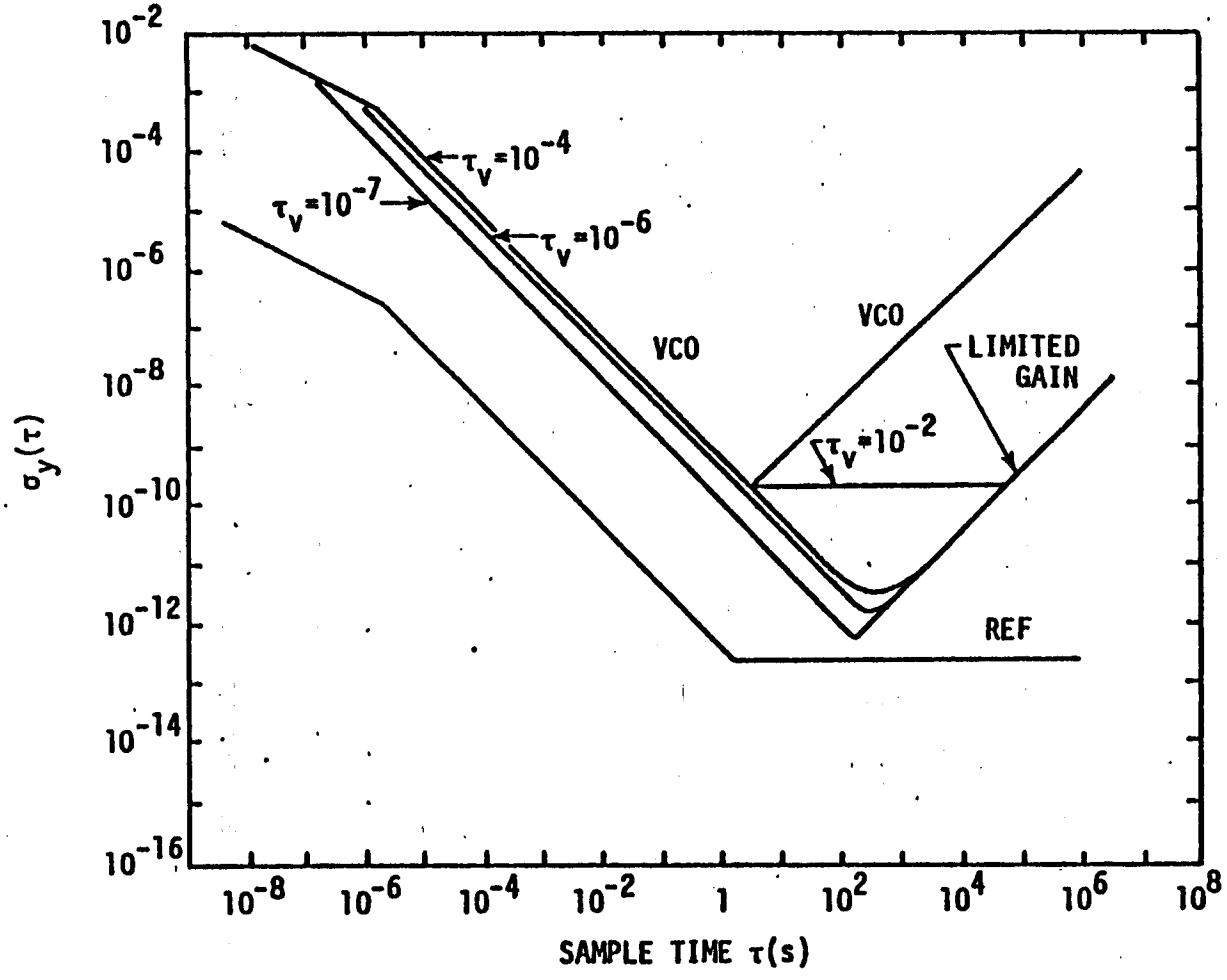
10^{-2}
10^{-4}
10^{-6}
10^{-8}
10^{-10}
10^{-12}
10^{-14}
10^{-16}
$\sigma_y(\tau)$
$\tau_v=10^{-4}$
$\tau_v=10^{-7}$
$\tau_v=10^{-6}$
VCO
VCO
LIMITED GAIN
$\tau_v=10^{-2}$
REF
10^{-8} 10^{-6} 10^{-4} 10^{-2} 1 10^{2} 10^{4} 10^{6} 10^{8}
SAMPLE TIME τ(s)

FIGURE 13

This example also illustrates that 6 dB per octave gain slope is not fast enough to correct for some of the divergent low frequency processes which are in many, indeed virtually all present oscillators.

Figure 14 shows more of a typical example, namely one in which the reference oscillator (curve b) has poor short-term stability (white phase noise) and flicker of frequency in long-term. The VCO (curve a), on the other hand, shows good short-term stability but drifts away rather rapidly. There are of course many ways to design the servo system gain in order to optimize the phase spectrum or time domain stability in the region of importance for a particular application. Assuming that we are interested in the optimum time domain stability rather than the direct phase spectrum, the servo gain slope shown in Figure 15 could be used. The gain crosses unity with a 6 dB/octave slope which results in a stable operating condition. At 1/4 the unity gain bandwidth or 4 times longer attack time, another integrator becomes active. The dotted line (curve c) of Figure 14 shows the resulting $S_\phi(f)$. Note that in contrast to the 6 dB/octave gain slope of Figure 12 that the 12 dB/octave gain slope is fast enough to substantially decrease the low frequency noise. The high frequency noise is degraded only slightly for frequencies above the unity gain point [1, 9].

Figure 16 shows the resulting time domain stability. Note that by removing the high frequency noise via the phase lock that the resulting system time domain stability reaches the flicker level much faster than for the reference alone. The servo gain slope of Figure 15 has one disadvantage and that is the need for gain stability. If the loop gain is lowered sufficiently the slope at unity gain approaches 12 dB/octave, then the system will most probably break into oscillation, on the other hand, an increase in loop gain over that shown in Figure 15 makes little difference in loop stability.

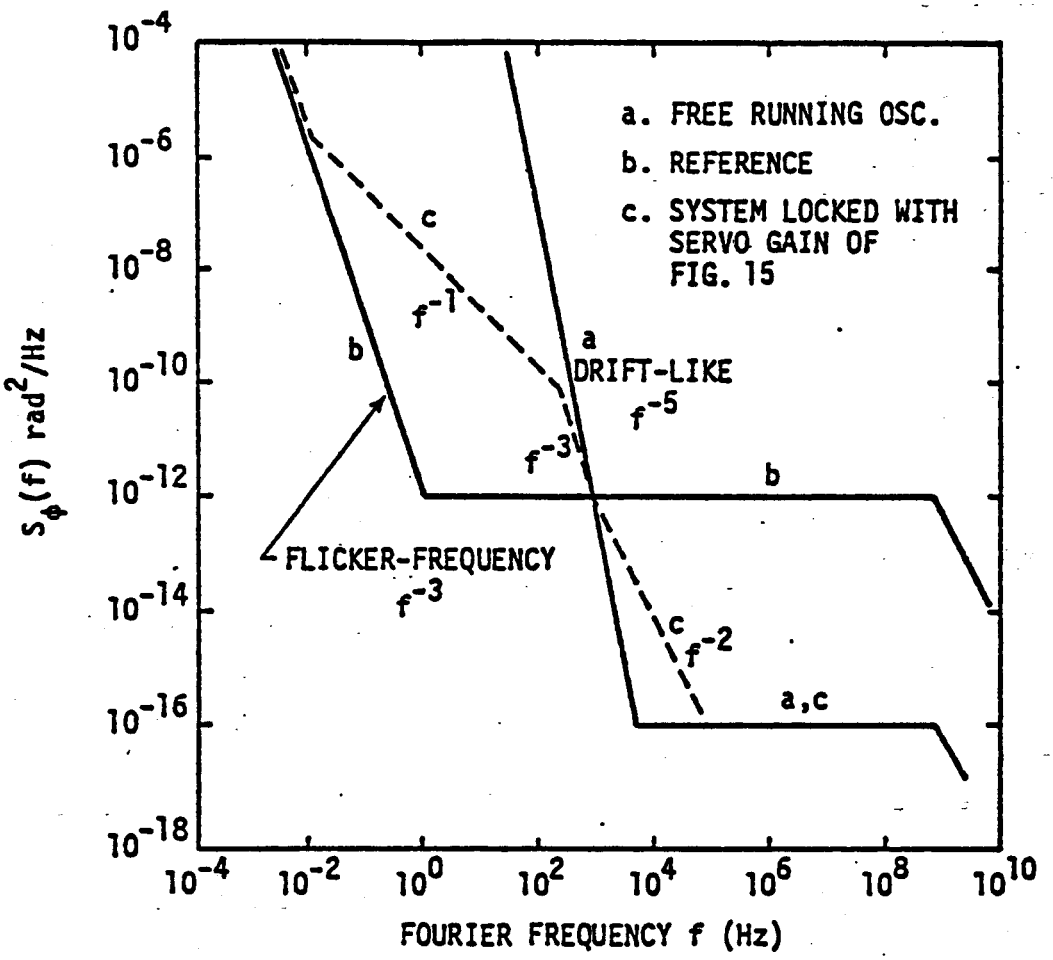
a. FREE RUNNING OSC.
b. REFERENCE
c. SYSTEM LOCKED WITH SERVO GAIN OF FIG. 15
a
DRIFT-LIKE
f^{-5}
b
c
f^{-1}
b
f^{-3}
FLICKER-FREQUENCY
f^{-3}
c
f^{-2}
a,c
$S_\phi(f)$ rad^2/Hz
10^{-4}
10^{-6}
10^{-8}
10^{-10}
10^{-12}
10^{-14}
10^{-16}
10^{-18}
10^{-4} 10^{-2} 10^{0} 10^{2} 10^{4} 10^{6} 10^{8} 10^{10}
FOURIER FREQUENCY f (Hz)

FIGURE 14

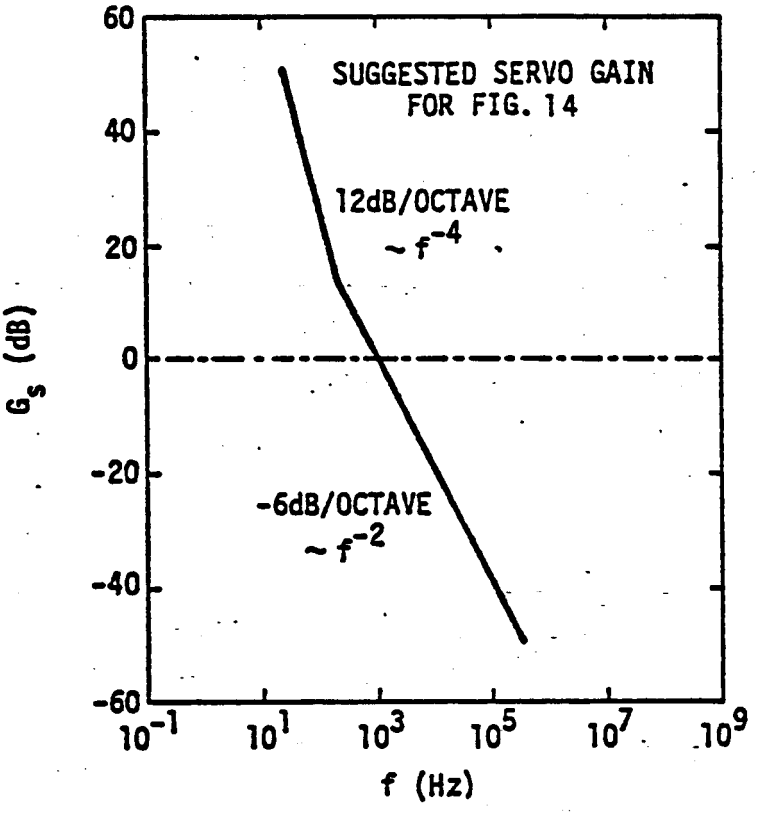

FIGURE 15

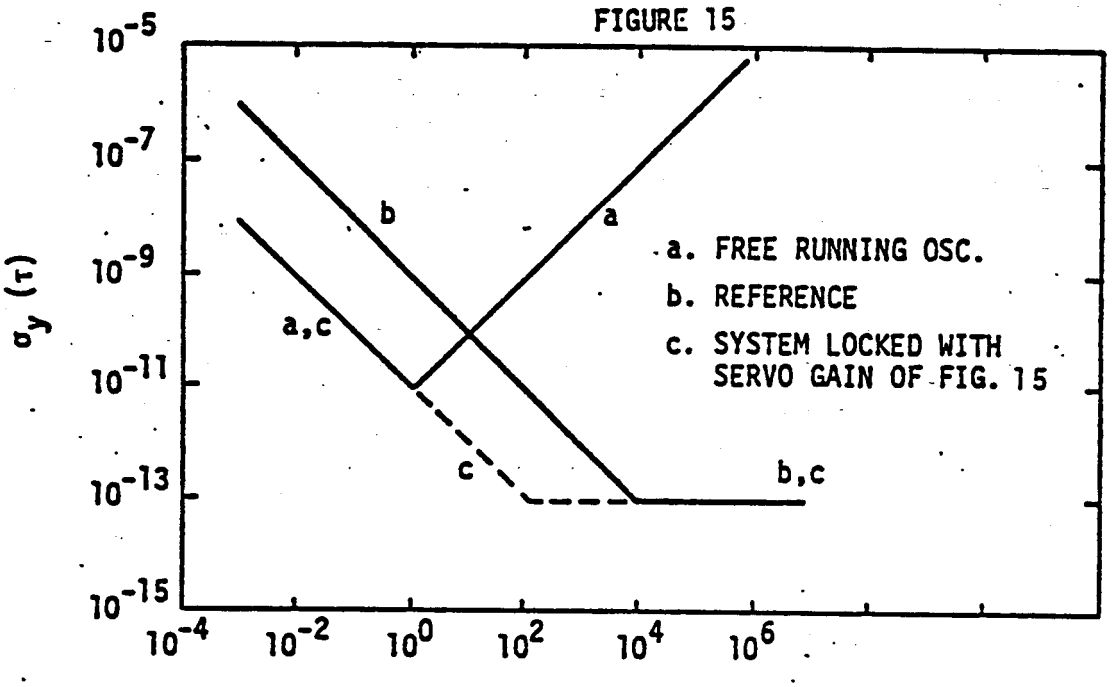

FIGURE 16

Figure 17 shows the time domain stability which can be achieved using a 6-12 dB servo gain slope as in Figure 15 to phase lock the two types of commercially available quartz oscillators typified by curves a & b of Figure 11. For comparison, the time domain stability of the Rb maser and the Stanford superconducting cavity system are also shown in Figure 17 [5]. The noise bandwidth is 1 kHz. One often sees time domain stability plots without the noise bandwidth being stated. While it is true that many of the frequency standards have noise processes which are supposed to lead to a time domain stability which is independent of bandwidth, the measurement systems and many of the ways we use frequency standards yield stabilities which do depend on the noise bandwidth.

So I think that it is important to note the bandwidth over which one measured the time domain stability. If $\sigma_y(\tau)$ is falling as $1/\tau$, or faster than $\tau^{-1/2}$, this is essential in order to obtain meaningful measurements.

I now would like to turn to the subject of frequency multiplication. It's well known that the effect of frequency multiplication on the phase spectral density is given by:

$$S_\phi(\nu, f) = n^2 S_\phi(\nu/n, f)$$

where n is the multiplication number. Recent analysis and some experimental checks have shown that the voltage spectral density such as you would observe on a power meter or spectrum analyzer is quite accurately given by following expressions [10]

$$S_v(f > f_o) = e^{-\phi_{f_o}(\nu)} [\delta_{f_o} + n^2 S_\phi(\nu/n, f)]$$

$$\phi_{f_o} \equiv \int_{f_o}^{\infty} S_\phi(\nu, f)\, df \text{ rad}^2.$$

One notes that when $\phi_{f_o} << 1$ that this expression reduces to the standard one,

$$S_v(f) = n^2 S_\phi(\nu/n, f).$$

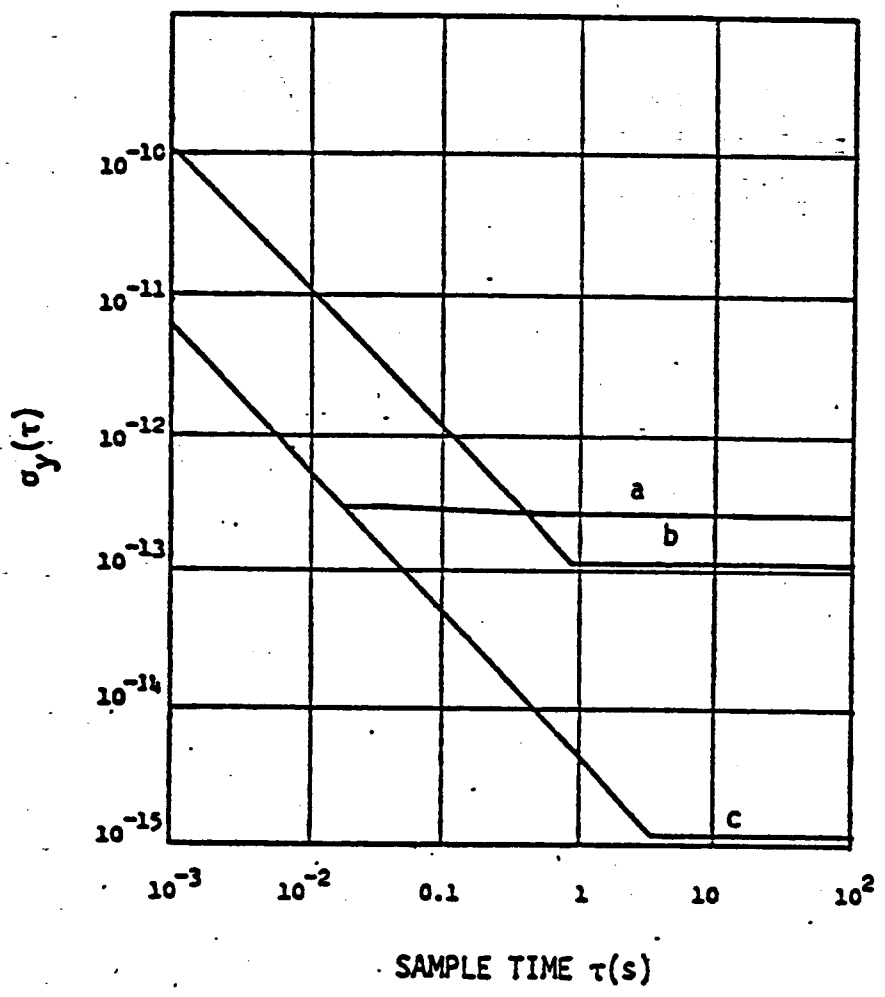
10^{-10}
10^{-11}
10^{-12}
10^{-13}
10^{-14}
10^{-15}
$\sigma_y(\tau)$
a
b
c
10^{-3}
10^{-2}
0.1
1
10
10^{2}
SAMPLE TIME τ(s)

FIGURE 17

The term $e^{-\phi}\ f_0(\nu)\ \delta f_0$ contains all the power in the frequency interval $\nu - f_0$ to $\nu + f_0$.

By appropriate choice of f_0 one can apply these two equations at particular points in the spectrum to predict the width of the carrier, the height of the carrier above the pedestal, the width of the pedestal, the point at which the signal disappears, within an accuracy of a few dB. This has been checked experimentally and in some specific cases, theoretically although to do it for all noise processes is a tough numerical job. Let us see how one would predict the amount of power left in the carrier after frequency multiplication. Let us pick a definition for the dividing line between the carrier and noise pedestal f_p, the point where the slope of $S_\phi(f)$ drops below f^{-1}. In this case, the relative power in the carrier after multiplication by a factor of n is just:

$$\text{Carrier Power} = e^{-\phi^p} \quad , \text{ where } \phi^p = \int_{f_p}^{\infty} S_\phi(f)\ df,$$

while the relative power in the noise pedestal is $1 - e^{-\phi^p}$. In most cases, changing the definition of f_p by a factor of 10 or 100 makes little difference since most of the phase modulation occurs at large Fourier frequencies.

Figure 18 illustrates the loss of power from the carrier as the phase modulation due to the pedestal, is increased. When ϕ^p is small compared to 1, the relative power in the carrier is independent of n, this corresponds to the standard equation, equating the phase and voltage spectral densities. However, as ϕ^p approaches 1 the carrier exponentially loses relative power. At some point, no matter how narrow a filter one uses, the density of power in the carrier is so small that one cannot distinguish it from the density of power in the pedestal shown in the lower curve. What does it mean for a real signal? Curve a, Figure 19 shows the voltage spectrum from a spectrum analyzer of the 5 MHz fundamental. The resolution is 10 kHz. Curve b shows the voltage spectrum at X-band; the signal-to-noise is still very good. Curve c shows the result at 500 GHz, the carrier is just a small peak and the pedestal width has started to grow. Curve d shows that at 1.5 THz that the carrier is totally gone. And that is in fact the result observed in many multiplication experiments - the signal-to-noise drops from some high value to zero after only a small increase in multiplication factor.

One can also predict the fast line width of the carrier as a function of multiplication factor by making use of the expression of power from $\nu - f_o$ to $\nu + f_o$:

$$\int_{\Delta\nu/2}^{\infty} S_\phi^c(\nu, f)df = \ln(2),$$

where S_ϕ^c is the carrier portion of the phase spectrum. There is a slight difference between this definition of carrier width via the 1/2 power points and the 3 dB intensity points. At most, the error is 3 dB in width and the difference is easily calculated if it's important [10]. For an oscillator exhibiting flicker of frequency in long-term, the fast carrier linewidth is closely given by:

$$\Delta\nu_c = 2\nu\sigma_y(\text{flicker}).$$

If one scans too slowly, the linewidth will appear to be increased over this due to the flicker process and if one goes too fast, the linewidth will be increased due to the windowing effect of the analyzer. Therefore, a certain amount of care must be taken in optimizing scan rate and bandwidth to observe this fast linewidth.

I will conclude with some predictions on frequency multiplication. The dotted line (Figure 20) shows the phase spectrum of the two 5 MHz quartz oscillators of Figure 11 locked together while the solid line shows the voltage spectrum after multiplication to 5 THz. (This frequency was chosen to overlap with some of the common FIR lasers.) These were calculated assuming noiseless multipliers. Note the linewidth of 3 Hz and the nearly 60 dB signal-to-noise in a 1-3 Hz bandwidth. Therefore one should expect to have at least 20 dB signal-to-noise in a 3 kHz bandwidth. Using the superconducting cavity as a source [6], one would predict a linewidth of ≈ 5 millihertz at 5 THz and signal-to-noise of beyond 60 dB even in a 1 kHz bandwidth. Even at 88 THz the superconducting cavity should have a linewidth of 0.1 Hz and a signal-to-noise greater than 30 dB in a 1 Hz bandwidth.

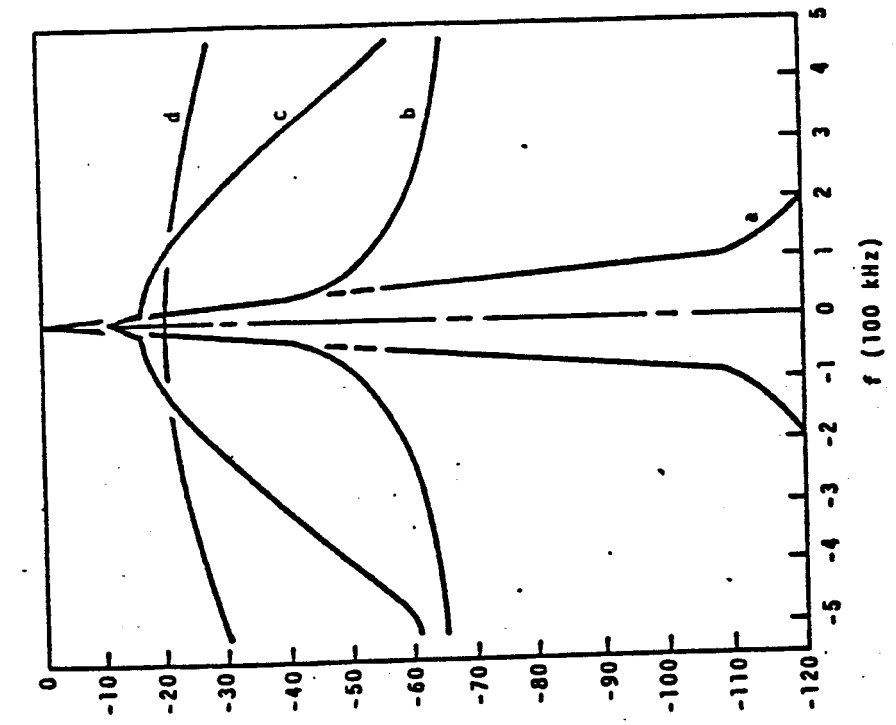

FIGURE 19

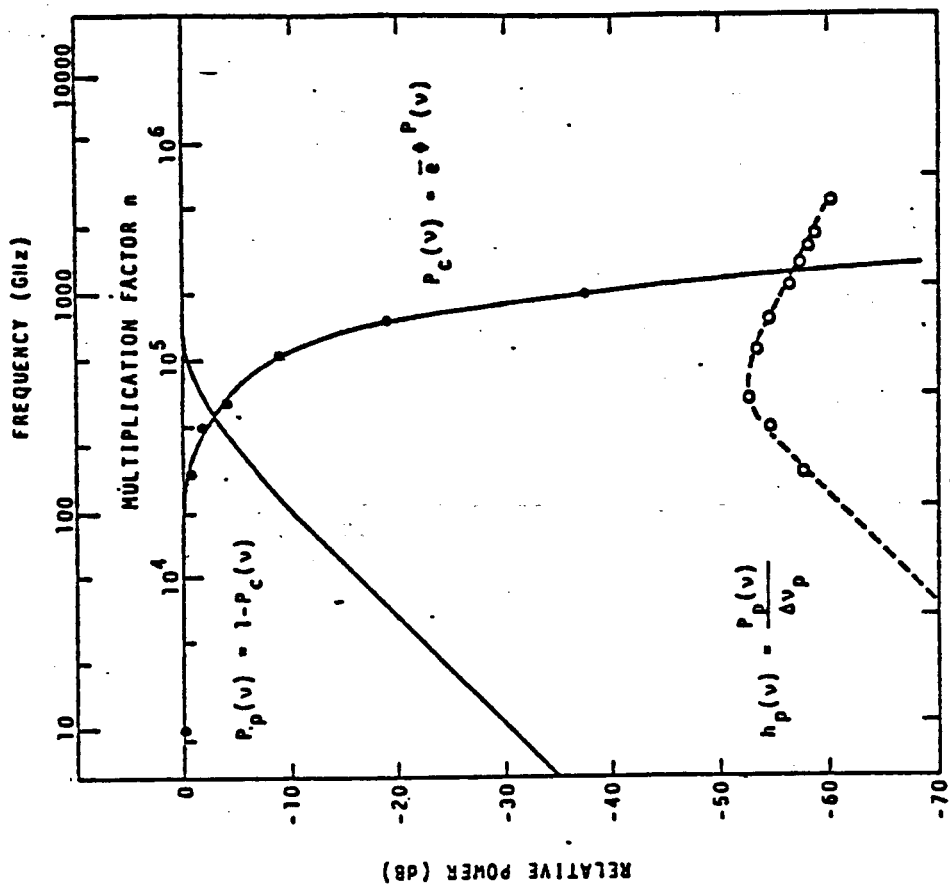

FIGURE 18

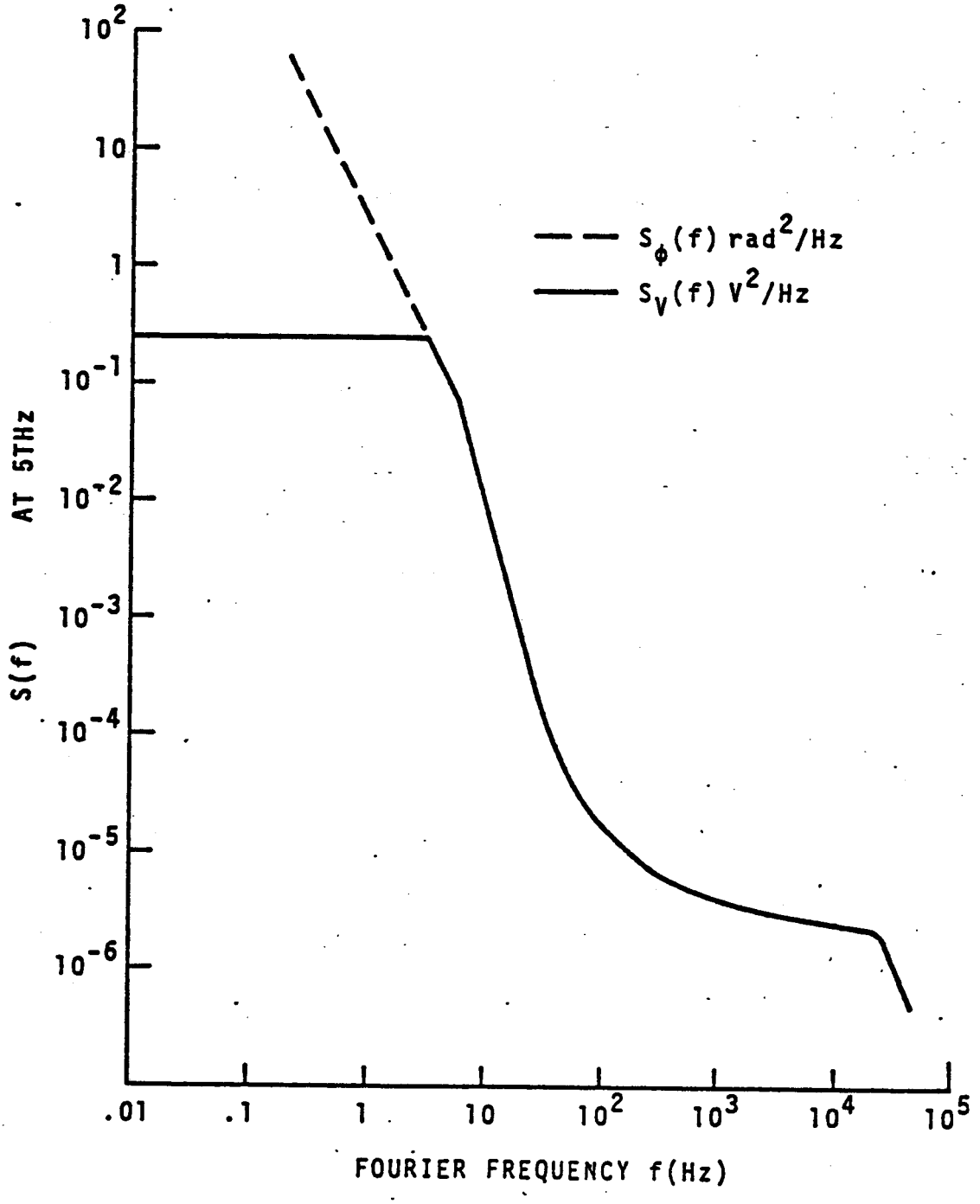
10^2
10
1
10^{-1}
10^{-2}
10^{-3}
10^{-4}
10^{-5}
10^{-6}
S(f)
AT 5THz
$S_\phi(f)$ rad^2/Hz
$S_V(f)$ V^2/Hz
.01
.1
1
10
10^2
10^3
10^4
10^5
FOURIER FREQUENCY f(Hz)

FIGURE 20

REFERENCES

[1] Design Considerations in State of the Art Signal Processing and Phase Noise Measurement System, F.L. Walls, S.R. Stein, J.E. Gray and D.J. Glaze, Proc. 30th Frequency Control Symposium, Atlantic City, NJ, 1976.

[2] Frequency Modulation Analysis with the Hadamard Variance, Proc. 25th Frequency Control Symposium, Atlantic City, NJ, 1971, pp. 222-225.

The Fast Fourier Transform, E.O. Brigham and R.E. Morrow, IEEE Spectrum 4, 12, Dec. 1967, pp. 63-70.

[3] A New Spectrum Analyzer using Both Analogue and Digital Filtering via the Hadamard Variance, V. Groslanbert, 1976 CPEM.

[4] Picosecond Time Difference Measurement Systems, D.W. Allan and Herman Daams, Proc. 29th Frequency Control Symposium, Atlantic City, NJ, 1975, pp. 404-411.

[5] The Development of the Superconducting Cavity Stabilized Oscillator, S.R. Stein and J.P. Turneaure, Proc. 27th Frequency Control Symposium, Atlantic City, NJ, 1973, pp. 414-420.

[6] A Superconducting Parametric Oscillator for use in Infrared Frequency Synthesis, S.R. Stein, 2nd Symp. on Frequency Standards and Metrology, Copper Mountain, CO, 1976.

[7] Short-term Frequency Stability of the Rb^{87} Maser, M. Tetu, Busca and J. Vanier. IEEE Trans. on I & M, IM-22, pp. 250-257, 1973. Also private communication.

[8] The exact expression is

$$\sigma_y^2(\tau) = \frac{2}{\tau^2}\frac{1}{\nu^2}\frac{1}{\pi^2}\int_0^{f_h} S_\phi(f)\sin^4(\pi f\tau)df$$

and was derived in, Some Aspects of the Theory and Measurement of Frequency Fluctuations in Frequency Standards, L.S. Cutler and C.L. Searle, Proc. IEEE 54, pp. 136-154, 1966.

[9] Phaselock Techniques, F.M. Gardner (John Wiley, New York, 1966).

Take the Guesswork out of Phase Locked Loop Design, D. Kesner, EDN, 5, pp. 54-60, January 1973.

[10] RF Spectrum of a Signal after Frequency Multiplication; Measurement and Comparison with a Simple Calculation, F.L. Walls and A. De Marchi. IEEE Trans. on I & M, IM-24, pp. 210-217, Sept. 1975.

FIGURE 1: Measured stabilities of several types of standards. The data are based on publications and specifications.

A: commercial Cs beam
B: commercial Rb gas cell
C: high performance commercial Cs beam
D: laboratory Cs beam
E: H maser (f_h = 10 Hz)
F: Rb maser, quartz oscillator (f_h = 1kHz)
G: quartz crystal controlled oscillator
G': new quartz crystal controlled oscillator (f_h = 1kHz)
H: Rb maser
J: SCC oscillator (f_h = 10 kHz)
K: CH_4 stabilizer laser

FIGURE 2: Typical system for measuring $S_\phi(f)$ of a pair of equal frequency oscillators. Noise floor for this system is shown in Figure 4.

FIGURE 3: Block diagram of a new spectrum analyzer using the Hadamard variance. This system automatically plots $S_\phi(f)$ for 16 different Fourier frequencies from 0.01 Hz to 1 kHz.

FIGURE 4: Typical measurement noise floor for $S_\phi(f)$ using the system illustrated in Figure 2 at 5 MHz. Similar performance is possible from 0.1 MHz to 1 GHz.

FIGURE 5: Block diagram of a new phase noise measurement system which is broadband and features low noise.

FIGURE 6: Block diagram of the hetrodyne or beat-frequency method of measuring time domain frequency stability. Measurement times limited to $\tau > \tau_b$. Typical noise floor shown in Figure 9, curve a.

FIGURE 7: Block diagram of tight phase lock method of measuring time domain frequency stability. Measurement times limited to $\tau > 1/(2\pi f_1)$ where f_1 is the unity gain bandwidth of the phase lock loop. Typical noise floor shown in Figure 9, curve a.

FIGURE 8: Block diagram of the dual mixer time difference method of measuring time domain frequency stability. Measurement times are typically limited by processing time to 0.002 seconds, although 10^{-6}s is possible. Typical noise floor shown in Figure 9, curve b.

FIGURE 9: Typical measurement floor for $\sigma_y(\tau)$ vs. τ for: a) hetrodyne and tight phase lock method and b) dual mixer time difference methos, Noise bandwidth is 1 kHz. See text for discussion on practical sample times.

FIGURE 10: A calculated $\sigma_y(\tau)$ vs. τ plot of white phase noise with some 60 Hz phase modulation superimposed. The power in the 60 Hz sidebands has been set equal to the power of the white phase noise in a 1 kHz bandwidth, f_h.

FIGURE 11: Spectral density of phase fluctuations, $S_\phi(f)$, for a number of oscillators. a. Commercial 5 MHz quartz oscillator; b. newly-available 5 MHz quartz oscillator; c. superconducting cavity stabilized oscillator operating at 10 GHz but referred to 5 MHz; d. rubidium maser.

FIGURE 12: Shows $S_\phi(f)$ for a VCO locked to a reference, as a function of the phase lock loop attack time, τ_v. Servo gain is assumed to vary as -6 dB/octave with a maximum gain of 10^4.

FIGURE 13: Time domain stability of the VCO and ref signals from Figure 12 for various phase lock loop attack times. Servo gain is assumed to vary as -6 dB/octave with a maximum gain of 10^4. Noise bandwidth $f_h = \infty$.

FIGURE 14: The dashed line shows the $S_\phi(f)$ which results from locking a free running oscillator typified by curve a to a reference typified by curve b, using the servo gain shown in Figure 15.

FIGURE 15: Suggested servo gain for Figure 14. This form of servo gain provides near optimal time domain performance for the system. See Figure 16.

FIGURE 16: Time domain stability calculated from $S_\phi(f)$ shown in Figure 14. Note that the time domain stability of the system is much better than either component between approximately 0.5 and 10^4 seconds. Noise bandwidth $f_h = \infty$.

FIGURE 17: Curve a) Time domain stability which results from phase locking two oscillators typified by curves a and b of Figure 11 with a servo gain shape similar to Figure 15. Curve b) Time domain stability of Rb maser [7]. Curve c) Time domain stability of superconducting cavity [5]. Noise bandwidth is 1 kHz.

FIGURE 18: The two solid curves illustrate the relative division of power between the carrier and noise pedestal as a function of ϕ^p, the phase modulation due to the noise pedestal. Also shown is the output frequency and multiplication factor corresponding to ϕ^p assuming a 5 MHz oscillator characterized by curve a, Figure 11. The lower dotted line shows the power density in the noise pedestal.

FIGURE 19: Relative power spectral density for a 5 MHz oscillator (curve a) after multiplication to (b) x band, (c) 500 GHz and (d) 1.5 THz. The resolution is 10 kHz. Note the relative loss of power from the carrier at 500 GHz and 1.5 THz, also the broadening of the noise pedestal.

FIGURE 20: Calculated spectral density of phase and voltage fluctuations at 5 THz for the 5 MHz oscillator system characterized by Figures 11 and 17. Note the predicted fast linewidth of 3 Hz.